

Poisson-Boltzmann formulary: Second edition

Cecilia Herrero^{1,*} and Laurent Joly^{2,†}

¹*Laboratoire Charles Coulomb (L2C), Université de Montpellier, CNRS, 34095 Montpellier, France*

²*Univ Lyon, Univ Claude Bernard Lyon 1, CNRS, Institut Lumière Matière, F-69622, VILLEURBANNE, France*

(Dated: October 13, 2022)

The Poisson-Boltzmann (PB) equation provides a mean-field theory of electrolyte solutions at interfaces and in confinement, with numerous applications ranging from colloid science to nanofluidics. This formulary gathers important formulas for the PB description of a $Z:Z$ electrolyte solution inside slit and cylindrical channels. Different approximated solutions (thin electrical double layers, no co-ion, Debye-Hückel, and homogeneous/parabolic potential limits) and their range of validity are discussed, together with the full solution for the slit channel. In addition, different boundary conditions are presented, the limits of the PB framework are briefly discussed, and Python scripts to solve the PB equation numerically are provided.

CONTENTS

I. Introduction	1	A. Thin EDL	9
II. Notations	2	B. Thick EDL, high surface charge: no co-ion	9
III. Characteristic lengths	2	1. PB equation: derivation	9
IV. Slit channel	3	2. PB equation: solution	10
A. Thin EDLs: one wall with salt	3	3. Surface charge and surface potential	10
1. PB equation: derivation	3	4. A few integrals	10
2. PB equation: solution	3	5. Low and high surface charge limits	10
3. Surface charge and surface potential	4	C. General case	11
4. A few integrals	4	1. Debye-Hückel limit	11
5. Thickness of the EDL	4	2. Homogeneous/parabolic potential limits	11
6. Low and high surface charge limits	4	3. No co-ion limit	11
B. Thick EDLs, high surface charge: two walls, no co-ion	5	D. Validity of the approximate solutions	12
1. PB equation: derivation	5	1. Thin EDL limit	12
2. PB equation: solution	5	2. Debye-Hückel limit	12
3. Surface charge and surface potential	6	3. Homogeneous/parabolic potential limits	12
4. A few integrals	6	4. No co-ion limit	13
5. Low and high surface charge limits	6	VI. Common boundary conditions	13
C. General case: two walls with salt	6	A. Surface charge density and surface potential	13
1. Exact solution	6	B. Constant charge	13
2. Debye-Hückel limit	7	C. Constant potential	13
3. Homogeneous/parabolic potential limits	7	D. Charge regulation	14
4. No co-ion limit	7	VII. Limits of the PB framework	14
D. Validity of the approximate solutions	8	Acknowledgments	14
1. Thin EDLs limit	8	References	14
2. Debye-Hückel limit	8	A. Numerical solution with Python	15
3. Homogeneous/parabolic potential limits	9	1. Slit channel	15
4. No co-ion limit	9	2. Cylindrical channel	16
V. Cylindrical channel	9		

I. INTRODUCTION

When an electrolyte solution meets a solid surface, several mechanisms can generate a surface charge, together with an opposite charge carried by ions in the liquid (typical mechanisms include dissociation of surface

* cecil.herr@gmail.com

† laurent.joly@univ-lyon1.fr

groups and specific adsorption of charged species) [1–3]. In the vicinity of a charged wall, ions reorganize to form a diffuse charged layer, the electrical double layer (EDL), which screens the surface electric field over the so-called Debye length denoted λ_D , see Fig. 1(a-b). The EDL plays a key role in many aspects of soft condensed matter, as it controls the stability and dynamics of charged objects in solution [1–3]. In particular, the EDL is at the origin of the so-called electrokinetic effects, where gradients and fluxes of different types (hydrodynamic, electrical, chemical, thermal) are coupled in the presence of charged interfaces [4]. Such electrokinetic effects are central to the very active field of nanofluidics [5–8].

The ion distribution and electric potential profile in the EDL can be computed by combining the Poisson equation for electrostatics and the Boltzmann distribution of the ions into the so-called Poisson-Boltzmann (PB) equation, under certain assumptions [9, 10]:

- the Poisson equation is written assuming that the solvent has a local, homogeneous and isotropic dielectric permittivity;
- the Boltzmann distribution of the ions is written assuming that the energy of the ions results only from their Coulomb interactions with the other ions and the wall, described at a mean-field level.

Educational presentations of the PB theory can be found in books [1–3], book chapters [9, 10], and articles [4], discussing in particular applications to nanofluidics [5–8].

In contrast, this formulary simply gathers important formulas for the description of the EDL with the PB equation, focusing on a $Z:Z$ electrolyte solution inside slit and cylindrical channels, see Fig. 1(c) and Fig. 1(d), respectively. After introducing the notations (Sec. II) and important characteristic lengths (Sec. III), the formulary describes the cases of a slit channel (Sec. IV) and of a cylindrical channel (Sec. V). For both geometries, different approximated solutions are discussed: the thin EDL limit, where λ_D is small as compared to the channel size; the no co-ion limit, where the EDLs overlap and the surface charge is large enough that co-ions are excluded; the Debye-Hückel limit at low surface charge, where the PB equation can be linearized. The range of validity of these approximations is then discussed; for the slit channel only, the general solution is presented. Finally the limits of the PB framework are briefly discussed in Sec. VII.

II. NOTATIONS

- solvent dielectric permittivity ϵ
- inverse thermal energy $\beta = 1/(k_B T)$, with k_B the Boltzmann constant and T the temperature

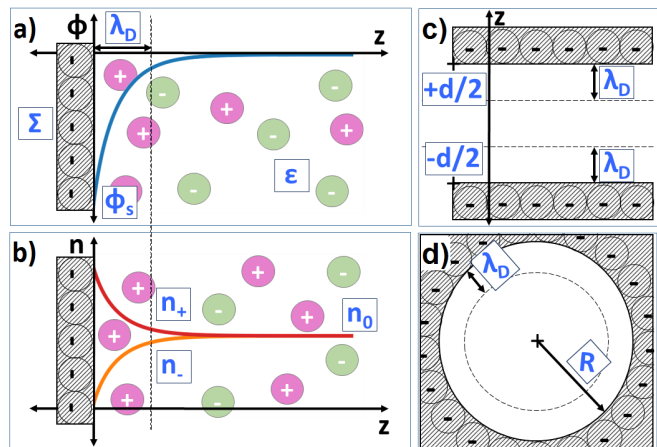


FIG. 1. a-b) Local picture of the electrical double layer at a charged wall (z is the distance from the wall, Σ the surface charge density, ϵ the solvent dielectric permittivity, and λ_D the Debye length): a) Profile of reduced electric potential ϕ , with ϕ_s the value at the wall; b) Profiles of cation n_+ and anion n_- densities, with n_0 the bulk value. c) Schematics of the slit channel. d) Schematics of the cylindrical channel.

- absolute ionic charge $q = Ze$, with e the elementary charge and Z the ion valence
- ion densities n_{\pm}
- charge density ρ_e
- salt concentration $n_0 = n_+ = n_-$ in the bulk/reservoirs
- surface charge density Σ
- electrostatic potential V
- reduced potential $\phi = \beta q V$
- their value at the wall V_s and ϕ_s
- auxiliary reduced potential $\psi = -\text{sgn}(\Sigma) \times \phi$
- Bjerrum length ℓ_B
- Debye length λ_D
- Gouy-Chapman length ℓ_{GC}
- $\chi = \lambda_D / \ell_{GC}$
- Dukhin length ℓ_{Du}

III. CHARACTERISTIC LENGTHS

Solvent permittivity ϵ : Bjerrum length ℓ_B – The Bjerrum length is the distance at which the electrostatic interaction energy between two ions is equal to the thermal energy $k_B T$.

$$\ell_B = \frac{\beta q^2}{4\pi\epsilon} \Leftrightarrow \epsilon = \frac{\beta q^2}{4\pi\ell_B} \quad (1)$$

For a monovalent salt in water at room temperature, $\ell_B \sim 0.7$ nm.

Bulk salt concentration n_0 : Debye length λ_D – The Debye length is the range of the exponential screening of the electric field in an electrolyte.

$$\lambda_D = \frac{1}{\sqrt{8\pi\ell_B n_0}} \Leftrightarrow n_0 = \frac{1}{8\pi\ell_B \lambda_D^2} \quad (2)$$

For a monovalent salt in water at room temperature, $\lambda_D \sim 0.3$ nm/ $\sqrt{n_0(\text{mol/L})}$.

Surface charge density Σ : Gouy-Chapman length ℓ_{GC} – The Gouy-Chapman length is the distance at which the electrostatic interaction energy between an ion and a charged surface is comparable to the thermal energy $k_B T$.

$$\ell_{GC} = \frac{q}{2\pi\ell_B |\Sigma|} \Leftrightarrow \Sigma = \text{sgn}(\Sigma) \frac{q}{2\pi\ell_B \ell_{GC}} \quad (3)$$

For monovalent ions in water at room temperature, $\ell_{GC} \sim 36$ nm/ $|\Sigma|(\text{mC/m}^2)$.

In the following, it will appear that many quantities can be expressed as a function of the ratio $\chi = \lambda_D/\ell_{GC}$, which is proportional to the absolute value of the surface charge, and inversely proportional to the square root of the bulk salt concentration:

$$\chi = \frac{\lambda_D}{\ell_{GC}} = 2\pi\ell_B \lambda_D \frac{|\Sigma|}{q} = \frac{|\Sigma|/q}{\sqrt{n_0}} \sqrt{\frac{\pi\ell_B}{2}}$$

Surface ions vs bulk ions: Dukhin length ℓ_{Du} – The Dukhin length is the channel scale at which the number of salt ions in bulk compares to the number of counterions at the surfaces [6].

$$\ell_{Du} = \frac{|\Sigma|/q}{n_0} \quad (4)$$

IV. SLIT CHANNEL

This section gathers the equations describing a $Z:Z$ electrolyte solution confined between two planar parallel walls at a distance d , see Fig. 1(c).

A. Thin EDLs: one wall with salt

When the distance d between the surfaces is much larger than the thickness of the EDLs, one can solve the PB equation for a single charged wall, and superimpose the potentials of the two walls to obtain the full potential in the channel. The limits of validity of this approximation will be quantified in section IV D.

Accordingly, this section gathers formulas for the description of a $Z:Z$ electrolyte solution in contact with a single planar wall, where $z \geq 0$ is the distance from the wall, see Fig. 1(a) and (b).

1. PB equation: derivation

Poisson equation:

$$-\varepsilon \frac{d^2 V}{dz^2} = \rho_e(z) = q\{n_+(z) - n_-(z)\}$$

Boltzmann distribution:

$$n_{\pm}(z) = n_0 \exp\{\mp\beta qV(z)\}$$

Poisson-Boltzmann equation

$$\frac{d^2 \phi}{dz^2} = \frac{1}{\lambda_D^2} \sinh\{\phi(z)\} \quad (5)$$

2. PB equation: solution

Multiplying both sides of Eq. (5) by $d\phi/dz$ and integrating between $z = \infty$ and z ; imposing that $d\phi/dz|_{z=\infty} = \phi(\infty) = 0$:

$$\frac{1}{2} \left(\frac{d\phi}{dz} \right)^2 = \frac{1}{\lambda_D^2} \{\cosh(\phi) - 1\} \quad (6)$$

Noting that $\cosh(\phi) - 1 = 2 \sinh^2(\phi/2)$, and that ϕ and $d\phi/dz$ are of opposite sign:

$$\frac{d\phi}{dz} = -\frac{2}{\lambda_D} \sinh\left(\frac{\phi}{2}\right) \quad (7)$$

Noting that $\sinh(\phi/2) = 2 \sinh(\phi/4) \cosh(\phi/4) = 2 \tanh(\phi/4) \cosh^2(\phi/4)$, and integrating like a physicist:

$$\begin{aligned} \int_{\phi_s}^{\phi} \frac{d(\phi/4)}{\tanh(\phi/4) \cosh^2(\phi/4)} &= - \int_0^z \frac{dz}{\lambda_D} \\ \Rightarrow \ln \left| \tanh\left(\frac{\phi}{4}\right) \right| - \ln \left| \tanh\left(\frac{\phi_s}{4}\right) \right| &= -\frac{z}{\lambda_D} \end{aligned}$$

Noting that ϕ and ϕ_s have the same sign:

$$\tanh\left(\frac{\phi}{4}\right) = \tanh\left(\frac{\phi_s}{4}\right) e^{-\frac{z}{\lambda_D}}$$

Noting that $\text{atanh}(x) = \frac{1}{2} \ln\left(\frac{1+x}{1-x}\right)$, and defining

$$\gamma = \tanh\left(\frac{\phi_s}{4}\right) \quad (8)$$

one finally gets:

$$\phi(z) = 4 \text{atanh} \left\{ \gamma e^{-\frac{z}{\lambda_D}} \right\} = 2 \ln \left(\frac{1 + \gamma e^{-\frac{z}{\lambda_D}}}{1 - \gamma e^{-\frac{z}{\lambda_D}}} \right) \quad (9)$$

3. Surface charge and surface potential

Electrostatics at the interface:

$$\begin{aligned} -\left. \frac{dV}{dz} \right|_{z=0} &= \frac{\Sigma}{\varepsilon} \\ \Rightarrow \left. \frac{d\phi}{dz} \right|_{z=0} &= -4\pi\ell_B \frac{\Sigma}{q} = -\frac{2\operatorname{sgn}(\Sigma)}{\ell_{GC}} \end{aligned} \quad (10)$$

Note that Eq. (10) also follows from the global electroneutrality of the system:

$$\int_0^\infty \rho_e dz = -\int_0^\infty \varepsilon \frac{d^2V}{dz^2} dz = \varepsilon \left. \frac{dV}{dz} \right|_{z=0} = -\Sigma$$

Using Eq. (7), one obtains *Grahame equation* relating ϕ_s and Σ :

$$\sinh\left(\frac{\phi_s}{2}\right) = 2\pi\ell_B\lambda_D \frac{\Sigma}{q} = \operatorname{sgn}(\Sigma)\chi \quad (11)$$

so that ϕ_s can be expressed as:

$$\begin{aligned} \phi_s &= 2\operatorname{sgn}(\Sigma) \operatorname{asinh}(\chi) \\ &= 2\operatorname{sgn}(\Sigma) \ln\left\{\chi + \sqrt{1+\chi^2}\right\} \end{aligned} \quad (12)$$

One can also express $\gamma = \tanh(\phi_s/4)$ as a function of Σ , or equivalently as a function of χ :

$$\gamma = \frac{\operatorname{sgn}(\Sigma)}{\chi} \left\{-1 + \sqrt{1+\chi^2}\right\} \quad (13)$$

4. A few integrals

a. Electrostatic energy \mathcal{E}

$$\begin{aligned} \mathcal{E} &= \frac{\varepsilon}{2} \int_0^\infty \left(\frac{dV}{dz}\right)^2 dz = \frac{1}{8\pi\ell_B\beta} \int_0^\infty \left(\frac{d\phi}{dz}\right)^2 dz \\ &= \frac{1}{2\pi\ell_B\lambda_D\beta} \left\{-1 + \sqrt{1+\chi^2}\right\} = \frac{|\gamma|}{2\pi\ell_B\ell_{GC}\beta} \end{aligned} \quad (14)$$

b. Ionic densities

o Total density excess

Using Eq. (6),

$$n_+ + n_- - 2n_0 = 2n_0 \{\cosh(\phi) - 1\} = \frac{1}{8\pi\ell_B} \left(\frac{d\phi}{dz}\right)^2$$

Therefore,

$$\int_0^\infty (n_+ + n_- - 2n_0) dz = \beta\mathcal{E} \quad (15)$$

o Density difference

Electroneutrality imposes that:

$$\int_0^\infty \rho_e(z) dz = -\Sigma$$

Remembering that $\rho_e = q(n_+ - n_-)$, one gets:

$$\int_0^\infty (n_+ - n_-) dz = -\frac{\Sigma}{q} = -\frac{\operatorname{sgn}(\Sigma)}{2\pi\ell_B\ell_{GC}} \quad (16)$$

c. More integrals

$$\begin{aligned} \mathcal{F} &= \int_0^\infty (\phi_s - \phi) \left(\frac{d\phi}{dz}\right)^2 dz \\ &= \frac{8\operatorname{sgn}(\Sigma)}{\lambda_D} \{\chi - \operatorname{asinh}(\chi)\} \end{aligned} \quad (17)$$

$$\mathcal{G} = \int_0^\infty z \left(\frac{d\phi}{dz}\right)^2 dz = -4 \ln(1 - \gamma^2) \quad (18)$$

5. Thickness of the EDL

The thickness of the EDL is often identified with the Debye length λ_D . However, at high $|\Sigma|$, the charge of the EDL is concentrated in a region much thinner than λ_D . The characteristic thickness of the charged region can be defined as:

$$\lambda = \frac{\int_0^\infty z \rho_e(z) dz}{\int_0^\infty \rho_e(z) dz} = \frac{\varepsilon V_s}{\Sigma} = \frac{V_s}{-\left. \frac{dV}{dz} \right|_{z=0}} = \frac{\phi_s}{-\left. \frac{d\phi}{dz} \right|_{z=0}}$$

Using Eq. (10) and Eq. (12), one gets:

$$\lambda = \lambda_D \frac{\operatorname{asinh}(\chi)}{\chi} = \ell_{GC} \operatorname{asinh}(\chi) \quad (19)$$

The characteristic scale for the variation of the electric field can also be written, following Weisbuch and Guéron [11]:

$$\lambda' = \frac{-\left. \frac{d\phi}{dz} \right|_{z=0}}{\left. \frac{d^2\phi}{dz^2} \right|_{z=0}} = \frac{\lambda_D}{\sqrt{1+\chi^2}} \quad (20)$$

The limits at low and high surface charge of these characteristic scales are reported in section IV A 6 c (Table I).

6. Low and high surface charge limits

a. *Critical surface charge* When the surface charge $|\Sigma|$ is low enough that the reduced potential $|\phi|$ is much lower than 1 everywhere, and therefore when $|\phi_s| =$

$\max(|\phi|) \ll 1$, the PB equation can be linearized; this is the Debye-Hückel (DH) regime.

Using Grahame equation, Eq. (11), it appears that this regime is found when $\chi = \lambda_D/\ell_{GC} \ll 1$. The related critical surface charge for which $\lambda_D = \ell_{GC}$ writes:

$$|\Sigma|_c = \frac{q}{2\pi\ell_B\lambda_D} = \sqrt{\frac{8\epsilon n_0}{\beta}} \quad (21)$$

For instance, for a monovalent salt in water at room temperature:

$$|\Sigma|_c \sim \frac{36 \text{ mC/m}^2}{\lambda_D(\text{nm})} \sim 120 \text{ mC/m}^2 \sqrt{n_0(\text{mol/L})} \quad (22)$$

In practice, the linearized equation only provides a fair description for $|\Sigma| \lesssim 0.2|\Sigma|_c = 24 \text{ mC/m}^2 \sqrt{n_0(\text{mol/L})}$. Thus, except at very high salt concentration, the DH regime is only found for very low surface charge.

b. Debye-Hückel regime When $\chi = \lambda_D/\ell_{GC} \ll 1$, the PB equation can be linearized and its solutions simplified:

- the PB equation becomes: $\frac{d^2\phi}{dz^2} = \frac{1}{\lambda_D^2}\phi$
- the potential becomes: $\phi(z) = \phi_s e^{-z/\lambda_D}$
- γ becomes $\phi_s/4$
- the Grahame relation becomes: $V_s/\lambda_D = \Sigma/\epsilon$

c. Some limits at low and high surface charge The limits of ϕ_s , γ , \mathcal{E} , λ , λ' , \mathcal{F} and \mathcal{G} at low and high surface charge are reported in Table I.

B. Thick EDLs, high surface charge: two walls, no co-ion

When the EDLs overlap and for large enough surface charges (these conditions will be quantified in section IV D), co-ions are excluded from the channel and the PB equation can be solved with counter-ions only.

1. PB equation: derivation

Let's consider counter-ions with density $n(z)$ confined between two parallel walls located at $z = -d/2$ and $z = d/2$, bearing the same surface charge density Σ .

In order to make the equations describing a negative surface charge (with positive counter-ions) or a positive surface charge (with negative counter-ions) identical, one can define an auxiliary reduced potential ψ , which will always be negative:

$$\psi = -\text{sgn}(\Sigma) \times \phi = -\text{sgn}(\Sigma) \times \beta q V. \quad (23)$$

Quantity	$\chi = \lambda_D/\ell_{GC} \ll 1$	$\chi = \lambda_D/\ell_{GC} \gg 1$
ϕ_s	$\text{sgn}(\Sigma)2\chi = \beta q \frac{\Sigma\lambda_D}{\epsilon}$	$2 \text{sgn}(\Sigma) \ln(2\chi)$
γ	$\text{sgn}(\Sigma)\frac{\chi}{2} = \beta q \frac{\Sigma\lambda_D}{4\epsilon}$	$\text{sgn}(\Sigma)$
\mathcal{E}	$\frac{\chi^2}{4\pi\beta\ell_B\lambda_D} = \frac{\Sigma^2\lambda_D}{4\epsilon}$	$\frac{\chi}{2\pi\beta\ell_B\lambda_D} = \frac{ \Sigma }{\beta q}$
λ	λ_D	$\ell_{GC} \ln(2\chi)$
λ'	λ_D	ℓ_{GC}
\mathcal{F}	$\frac{4 \text{sgn}(\Sigma)\chi^3}{3\lambda_D}$	$\frac{8 \text{sgn}(\Sigma)\chi}{\lambda_D}$
\mathcal{G}	χ^2	$4 \ln\left(\frac{\chi}{2}\right)$

TABLE I. One wall with salt: limits of ϕ_s , γ , \mathcal{E} , λ , λ' , \mathcal{F} and \mathcal{G} for $\chi = \lambda_D/\ell_{GC} \ll 1$ (low surface charge, DH regime) and for $\chi = \lambda_D/\ell_{GC} \gg 1$ (high surface charge regime).

The potential in the middle of the channel is arbitrarily fixed to zero: $\psi_m = \psi(z=0) = 0$ (this condition will be relaxed in section IV C 4). Denoting n_m the counter-ion density at $z = 0$, and introducing a new characteristic length K^{-1} ,

$$K^{-1} = \frac{1}{\sqrt{2\pi\ell_B n_m}} \Leftrightarrow n_m = \frac{K^2}{2\pi\ell_B}, \quad (24)$$

one can derive the PB equation.

Poisson equation:

$$qn(z) = -\frac{\epsilon}{\beta q} \frac{d^2\psi}{dz^2}$$

Boltzmann distribution:

$$n(z) = n_m e^{-\psi(z)}$$

Poisson-Boltzmann equation:

$$\frac{d^2\psi}{dz^2} = -2K^2 e^{-\psi(z)} \quad (25)$$

2. PB equation: solution

$$\psi(z) = \ln\{\cos^2(Kz)\} \quad (26)$$

$$\frac{d\psi}{dz} = -2K \tan(Kz) \quad (27)$$

$$n(z) = \frac{n_m}{\cos^2(Kz)} = \frac{K^2}{2\pi\ell_B \cos^2(Kz)} \quad (28)$$

3. Surface charge and surface potential

To fully determine the potential and ion density profiles, one needs to express K as a function of the surface charge.

Electrostatics at the interface (or equivalently, global electroneutrality):

$$\left. \frac{dV}{dz} \right|_{z=d/2} = \frac{\Sigma}{\varepsilon} \Rightarrow \left. \frac{d\psi}{dz} \right|_{z=d/2} = -\frac{2}{\ell_{GC}} \quad (29)$$

Using Eq. (27), one obtains:

$$Kd \tan\left(\frac{Kd}{2}\right) = \frac{d}{\ell_{GC}}. \quad (30)$$

Equation (30) only provides an implicit expression for K , but a very accurate explicit approximation (error below 0.07%) can be written:

$$\frac{Kd}{2} \approx \frac{\pi}{2} \sqrt{\frac{x(x+5)}{x^2+9x+5\pi^2/2}}, \quad (31)$$

with $x = d/\ell_{GC}$.

Simpler approximate expressions can also be derived in the low and high surface charge limits, see Sec. IV B 5.

4. A few integrals

a. Electrostatic energy \mathcal{E}

$$\begin{aligned} \mathcal{E} &= \frac{\varepsilon}{2} \int_{-d/2}^{d/2} \left(\frac{dV}{dz} \right)^2 dz \\ &= \frac{2}{\pi d \ell_B \beta} \frac{Kd}{2} \left[\tan\left(\frac{Kd}{2}\right) - \frac{Kd}{2} \right] \end{aligned} \quad (32)$$

An approximate expression as a function of $x = d/\ell_{GC}$ (error below 1%) can be written:

$$\mathcal{E} \approx \frac{1}{\pi d \ell_B \beta} \times \frac{x^2}{6 - \sqrt{x/5} + x}. \quad (33)$$

b. Ionic density

$$\int_{-d/2}^{d/2} n(z) dz = \frac{2|\Sigma|}{q} = \frac{1}{\pi \ell_B \ell_{GC}} \quad (34)$$

5. Low and high surface charge limits

a. Low surface charge When Σ is small enough that $d/\ell_{GC} \ll 1$, Eq. (30) simplifies:

$$Kd \approx \sqrt{2d/\ell_{GC}}, \quad (35)$$

which is accurate within 1% up to $d/\ell_{GC} \approx 0.12$.

Note that when $d/\ell_{GC} \ll 1$, $Kd \ll 1$, so that $\psi \approx 0$ and the ion density is approximately homogeneous in the channel:

$$n \approx \frac{K^2}{2\pi \ell_B} = \frac{1}{\pi d \ell_B \ell_{GC}}. \quad (36)$$

This is commonly called the *ideal gas* regime. In practice, the ion density varies by less than 10% over the channel thickness as long as $d/\ell_{GC} < 0.2$.

b. High surface charge When Σ is large enough that $d/\ell_{GC} \gg 1$, Eq. (30) simplifies:

$$Kd \approx \frac{\pi}{1 + \frac{2\ell_{GC}}{d}}, \quad (37)$$

which is accurate within 1% down to $d/\ell_{GC} \approx 7$.

Eventually, when $d/\ell_{GC} \rightarrow \infty$, $Kd \rightarrow \pi$, and the potential and ion density profiles reach a limit, sometimes referred to as the ‘‘Gouy-Chapman limit’’:

$$\psi(z) = \ln \{ \cos^2(\pi z/d) \} \quad (38)$$

$$n(z) = \frac{\pi}{2d^2 \ell_B \cos^2(\pi z/d)} \quad (39)$$

C. General case: two walls with salt

1. Exact solution

In the general case of an aqueous electrolyte confined between two symmetrical parallel walls located at $z = -d/2$ and $z = d/2$, the potential profile can be written in terms of the Jacobi elliptic functions cd , sn , cn and dn .

As for the no co-ion regime (see Sec. IV B), one can define an auxiliary reduced potential ψ , which is always negative:

$$\psi = -\text{sgn}(\Sigma) \times \phi = -\text{sgn}(\Sigma) \times \beta q V. \quad (40)$$

The auxiliary potential writes:

$$\psi(y) = 2 \ln \left\{ \sqrt{m} \text{cd} \left(\frac{y r_1}{2\sqrt{m}}, m^2 \right) \right\}, \quad (41)$$

where $y = z/d \in [-0.5; 0.5]$ is the reduced position, $r_1 = d/\lambda_D$, and $m = \exp(\psi_m)$ with ψ_m the potential in the middle of the slab. The parameter m is the solution of:

$$r_2 = \frac{1 - m^2}{2\sqrt{m}} \times \frac{\text{sn} \left(\frac{r_1}{4\sqrt{m}}, m^2 \right)}{\text{cn} \left(\frac{r_1}{4\sqrt{m}}, m^2 \right) \text{dn} \left(\frac{r_1}{4\sqrt{m}}, m^2 \right)}, \quad (42)$$

where $r_2 = \lambda_D/\ell_{GC}$. For a given r_1 , m lies in the interval $]m_0, 1[$, where m_0 the solution of $4\sqrt{m}K(m^2) = r_1$ (with $K(x)$ the complete elliptic integral of the first kind).

The PB equation can also be solved numerically (a Python script to that aim is provided in the appendix, A 1), and different approximate solutions for the auxiliary reduced potential ψ expressed as a function of the reduced position $y = z/d$ can be written depending on r_1 and r_2 , discussed in the following.

2. Debye-Hückel limit

When the reduced potential $|\psi|$ is small everywhere (this condition will be quantified in section IV D), the PB equation can be linearized (DH regime, already encountered when considering only one wall in Sec. IV A).

With the conditions:

$$\left. \frac{d\psi}{dz} \right|_{z=0} = 0 \quad \text{and} \quad \left. \frac{d\psi}{dz} \right|_{z=d/2} = -\frac{2}{\ell_{GC}},$$

the solution to the linearized PB equation, $\frac{d^2\psi}{dz^2} = \psi/\lambda_D^2$, writes:

$$\psi = -\frac{2\lambda_D}{\ell_{GC}} \frac{\cosh\left(\frac{z}{\lambda_D}\right)}{\sinh\left(\frac{d}{2\lambda_D}\right)} = -2r_2 \frac{\cosh(yr_1)}{\sinh\left(\frac{r_1}{2}\right)}. \quad (43)$$

The corresponding potential V writes:

$$V(z) = \frac{\Sigma\lambda_D}{\varepsilon} \frac{\cosh\left(\frac{z}{\lambda_D}\right)}{\sinh\left(\frac{d}{2\lambda_D}\right)}. \quad (44)$$

The limits of validity of this approximation will be discussed in section IV D.

3. Homogeneous/parabolic potential limits

a. Homogeneous potential When the EDLs overlap ($r_1 = d/\lambda_D \ll 1$) and for low enough surface charges ($r_1 r_2 = d/\ell_{GC} \ll 1$), the potential and ion densities are almost homogeneous: this is commonly referred to as the ideal gas limit. In this limit, the ion densities and the auxiliary reduced potential write [6]:

$$n_{\pm}^{\text{IG}} = \mp \frac{\Sigma}{qd} + \sqrt{n_0^2 + \left(\frac{\Sigma}{qd}\right)^2} \quad (45)$$

$$= n_0 \left\{ \mp \text{sgn}(\Sigma) \frac{\ell_{\text{Du}}}{d} + \sqrt{1 + \left(\frac{\ell_{\text{Du}}}{d}\right)^2} \right\},$$

$$\psi_{\text{IG}} = -\text{asinh}\left(\frac{\ell_{\text{Du}}}{d}\right) = -\text{asinh}\left(\frac{4r_2}{r_1}\right), \quad (46)$$

introducing the Dukhin length $\ell_{\text{Du}} = (|\Sigma|/q)/n_0 = 4\lambda_D^2/\ell_{GC}$. An example of potential profile in the ideal gas regime is shown in Fig. 3. The limits of validity of this approximation will be discussed in section IV D.

b. Parabolic potential For weaker EDL overlaps, one can expand the solution of the PB equation in series of z/λ_D ; to second order, one obtains [12]:

$$\psi(z) \approx \psi_m + \frac{\sinh(\psi_m)}{2} \left(\frac{z}{\lambda_D}\right)^2. \quad (47)$$

Using $\psi_m = \psi_{\text{IG}}$, one gets:

$$\psi(z) \approx -\text{asinh}\left(\frac{4r_2}{r_1}\right) - \frac{2r_2}{r_1} \left(\frac{z}{\lambda_D}\right)^2. \quad (48)$$

However, the ideal gas potential is close to the average potential in the channel, and systematically shifted from the potential in the middle of the channel. The shift can be estimated as:

$$\frac{2}{d} \int_0^{d/2} -\frac{2r_2}{r_1} \left(\frac{z}{\lambda_D}\right)^2 dz \approx -\frac{r_1 r_2}{6},$$

and it can be subtracted from ψ_{IG} to obtain a closer approximation to ψ_m :

$$\psi_{\text{IG}}^{\text{cor}} = -\text{asinh}\left(\frac{4r_2}{r_1}\right) + \frac{r_1 r_2}{6}. \quad (49)$$

Overall, a good practical approximation for $\psi(z)$ is:

$$\begin{aligned} \psi(z) &\approx \psi_{\text{IG}}^{\text{cor}} + \frac{\sinh(\psi_{\text{IG}})}{2} \left(\frac{z}{\lambda_D}\right)^2 \\ &\approx -\text{asinh}\left(\frac{4r_2}{r_1}\right) + \frac{r_1 r_2}{6} - \frac{2r_2}{r_1} \left(\frac{z}{\lambda_D}\right)^2 \\ &\approx -\text{asinh}\left(\frac{4r_2}{r_1}\right) + \frac{r_1 r_2}{6} - 2r_1 r_2 y^2. \end{aligned} \quad (50)$$

An example of potential profile in the parabolic potential regime is shown in Fig. 3. The limits of validity of this approximation will be discussed in section IV D.

4. No co-ion limit

When the EDLs overlap and for large enough surface charges, co-ions are excluded from the channel and the PB equation can be solved with counter-ions only, see Sec. IV B. The auxiliary reduced potential $\psi(r)$ and the counter-ion density profile $n(r)$ were given by Eq. (26) and by Eq. (28), respectively. Both ψ and n depended on an inverse length K related to the surface charge via Eq. (30).

However, the potential in the middle of the channel was arbitrarily fixed to zero. To reproduce the exact potential, one needs to acknowledge that the channel is connected to an external salt reservoir with salt concentration n_0 and corresponding Debye length λ_D . Moving the reference of potential to the reservoir, $\psi_0 = 0$, the Boltzmann distribution for the counter-ions becomes $n(z) = n_0 e^{-\psi(z)}$, and the PB equation rewrites:

$$\frac{d^2\psi}{dz^2} = -\frac{1}{2\lambda_D^2} e^{-\psi(z)},$$

$$\text{with } \left. \frac{d\psi}{dz} \right|_{z=0} = 0 \text{ and } \left. \frac{d\psi}{dz} \right|_{z=d/2} = -\frac{2}{\ell_{GC}}.$$

Denoting $Kd = r_3$, the solution writes:

$$\psi = 2 \ln \left[\frac{r_1}{2r_3} \cos(r_3 y) \right], \quad (51)$$

with

$$r_3 \tan \left(\frac{r_3}{2} \right) = r_1 r_2. \quad (52)$$

In particular, the potential in the center of the channel is $\psi_m = \psi(y=0) = 2 \ln [r_1/(2r_3)]$. An example of potential profile in the no co-ion regime is shown in Fig. 3. The limits of validity of this approximation will be discussed in section IV D.

D. Validity of the approximate solutions

In section IV C, it appeared that the potential profile is uniquely determined by the two ratios $r_1 = d/\lambda_D$ and $r_2 = \lambda_D/\ell_{GC}$. Here we will discuss the range of r_1 and r_2 where the different approximate solutions presented in the previous sections can safely be used. Following Markovich *et al.* [10], we will illustrate the domains of validity of the approximate solutions in a r_2 - r_1 diagram, see Fig. 2. Typical potential profiles corresponding to a strong EDL overlap are represented in Fig. 3, where the exact solution is compared to the approximated formulas.

1. Thin EDLs limit

When the distance d between the surfaces is much larger than the Debye length (corresponding to well-separated EDLs), one can solve the PB equation for a single charged wall (see Sec. IV A), and superimpose the potentials of the two walls to obtain the full potential in the channel.

In practice, this approach provides an accurate representation of the exact solution as long as $r_1 = d/\lambda_D > 5$. This boundary is represented with a green dashed line in Fig. 2.

2. Debye-Hückel limit

In practice, the DH potential introduced in Sec. IV C 2 is an excellent approximation to the exact potential as long as the surface potential, $|\psi_s| = \max(|\psi|) = |\psi(y=1/2)|$, remains under a (somehow arbitrary) critical value $\psi_c = 0.4$. This corresponds to $r_2 \leq \tanh(r_1/2) \times \psi_c/2$. This boundary is represented with a blue dashed line in Fig. 2.

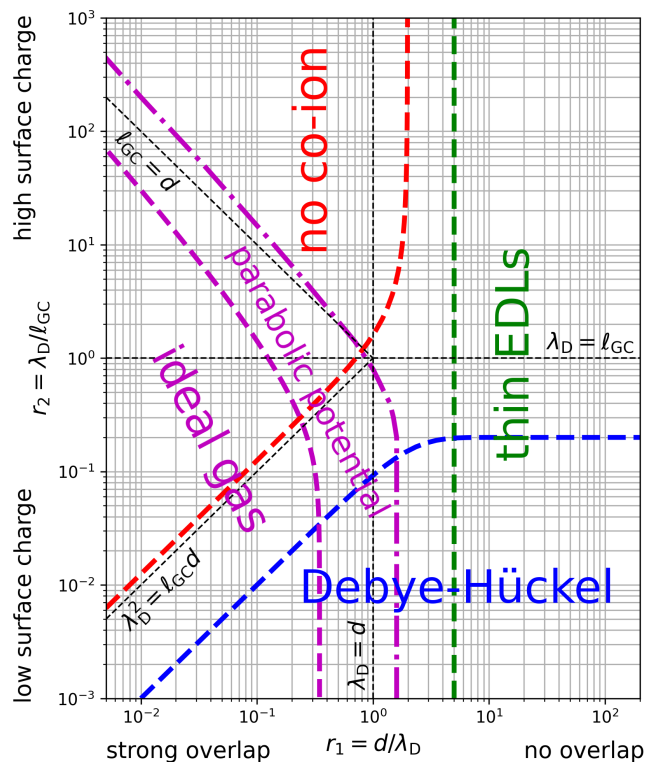


FIG. 2. Domains of validity of the different approximate solutions to the PB equation for an electrolyte solution confined between two planar walls, as a function of the ratios $r_1 = d/\lambda_D$ and $r_2 = \lambda_D/\ell_{GC}$, where d is the distance between the walls, λ_D the Debye length, and ℓ_{GC} the Gouy-Chapman length.

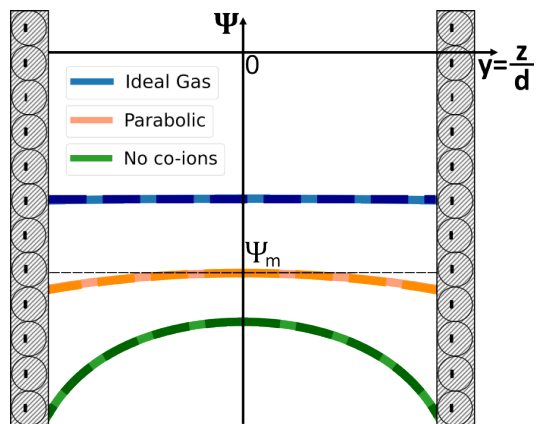


FIG. 3. Typical potential profiles for an electrolyte solution confined between two planar walls, in the strong overlap regime ($r_1 = d/\lambda_D = 0.1$). Three limiting regimes are illustrated: ideal gas/homogeneous potential ($r_2 = \lambda_D/\ell_{GC} = 1$), parabolic potential ($r_2 = 10$), and no co-ion ($r_2 = 100$) limits. In the three cases, the exact potential (light continuous line) is compared to the approximated formula for the ideal gas, Eq. (46), parabolic potential, Eq. (50), and no co-ion, Eq. (51), limits.

One can then simplify the relation between r_1 and r_2 by considering two limits: for thin EDLs, $r_1 \gg 1$, the DH solution can be used up to $r_2 \leq \psi_c/2$; for overlapping EDLs, $r_1 \ll 1$, the DH solution can be used up to $r_2 \leq r_1 \times \psi_c/4$.

3. Homogeneous/parabolic potential limits

a. Homogeneous potential (ideal gas) To estimate the range of validity of the homogeneous potential approximation (see Sec. IV C 3), one can compare the homogeneous potential value to the next term in a Taylor series of the potential as a function of z/λ_D , i.e., the parabolic term.

The homogeneous potential writes: $|\psi_{IG}| = \text{asinh}(4r_2/r_1)$, and the maximum difference between the parabolic term and its average value writes: $r_1 r_2/3$. Imposing a maximum ratio θ_c between the two terms, one obtains:

$$r_1 r_2 = 3\theta_c \text{asinh}\left(\frac{4r_2}{r_1}\right). \quad (53)$$

This boundary is represented for $\theta_c = 1\%$ with a purple dashed line in Fig. 2.

b. Parabolic potential The accuracy of the parabolic potential approximation depends crucially on the choice of ψ_m . Using $\psi_m = \psi_{IG}$, the error is approximately half the one of the homogeneous potential approximation, which does not extend much the range of parameters where it can be applied. In contrast, Eq. (50) approximates the exact potential within 1% over a broader range of parameters, see the purple dashed-dotted line in Fig. 2.

4. No co-ion limit

To determine the limits of applicability of this regime, one can estimate the ratio η between counter-ions and co-ion densities in the middle of the channel:

$$\eta = \frac{n_m^{\text{counter-ion}}}{n_m^{\text{co-ion}}} = \exp\{-2\psi_m\} = \left(\frac{2r_3}{r_1}\right)^4. \quad (54)$$

One can consider that co-ions are efficiently excluded from the channel when η is above a critical value η_c , that we will arbitrarily fix to 100. Combining Eq. (52) and Eq. (54), one can see that $\eta = \eta_c$ corresponds to:

$$r_2 = \frac{\eta_c^{1/4}}{2} \tan\left(\frac{r_1 \eta_c^{1/4}}{4}\right). \quad (55)$$

This boundary is represented with a red dashed line in Fig. 2.

One can simplify the relation between r_1 and r_2 by considering two limits: for small surface charges, $r_2 \ll$

1, the no co-ion approximation can be used for $r_2 \geq r_1 \eta_c^{1/2}/8 \approx 1.25r_1$; for large surface charges, $r_2 \gg 1$, the no co-ion approximation can be used for $r_1 \leq 2\pi/\eta_c^{1/4} \approx 1.99$.

V. CYLINDRICAL CHANNEL

This section gathers the equations describing a $Z:Z$ electrolyte solution confined inside a cylindrical channel of radius R , see Fig. 1(d). More detailed discussions can be found in e.g. Refs. 13–15.

A. Thin EDL

When the channel radius R is much larger than the thickness of the EDL, one can neglect the wall curvature at the scale of the EDL, and solve the PB equation for a single planar charged wall, see section IV A, where the distance to the wall is $z = R - r$.

Accordingly, the integrals computed per unit surface for a single planar wall in Sec. IV A 4 can simply be multiplied by $2\pi R$ to obtain the corresponding integral per unit length of the cylindrical channel.

The limits of validity of this approximation will be quantified in section V D.

B. Thick EDL, high surface charge: no co-ion

When the EDLs overlap and for large enough surface charges (these conditions will be quantified in section V D), co-ions are excluded from the channel and the PB equation can be solved with counter-ions only.

1. PB equation: derivation

As for the slit channel, the counter-ion density is denoted $n(r)$, and one can define an auxiliary reduced potential ψ , which is always negative:

$$\psi = -\text{sgn}(\Sigma) \times \phi = -\text{sgn}(\Sigma) \times \beta q V.$$

The potential in the middle of the channel is arbitrarily fixed to zero: $\psi_m = \psi(r=0) = 0$ (this condition will be relaxed in section V C 3). Denoting n_m the counter-ion density at $r=0$, one can define the same characteristic length K^{-1} as for the slit geometry,

$$K^{-1} = \frac{1}{\sqrt{2\pi\ell_B n_m}} \Leftrightarrow n_m = \frac{K^2}{2\pi\ell_B},$$

and derive the PB equation for a negative surface charge (with positive counter-ions) or for a positive surface charge (with negative counter-ions).

Poisson equation:

$$qn(r) = -\frac{\varepsilon}{\beta q} \frac{1}{r} \frac{d}{dr} \left(r \frac{d\psi}{dr} \right)$$

Boltzmann distribution:

$$n(r) = n_m e^{-\psi(r)}$$

Poisson-Boltzmann equation:

$$\frac{1}{r} \frac{d}{dr} \left(r \frac{d\psi}{dr} \right) = -2K^2 e^{-\psi(r)} \quad (56)$$

2. PB equation: solution

$$\psi(r) = 2 \ln \left[1 - \left(\frac{Kr}{2} \right)^2 \right] \quad (57)$$

$$\frac{d\psi}{dr} = \frac{-K^2 r}{1 - \left(\frac{Kr}{2} \right)^2} \quad (58)$$

$$n(r) = \frac{n_m}{\left[1 - \left(\frac{Kr}{2} \right)^2 \right]^2} = \frac{K^2}{2\pi\ell_B \left[1 - \left(\frac{Kr}{2} \right)^2 \right]^2} \quad (59)$$

3. Surface charge and surface potential

To fully determine the potential and ion density profiles, one needs to express K as a function of the surface charge.

Electrostatics at the interface (or equivalently, global electroneutrality):

$$\left. \frac{dV}{dr} \right|_{r=R} = \frac{\Sigma}{\varepsilon} \Rightarrow \left. \frac{d\psi}{dr} \right|_{r=R} = -\frac{2}{\ell_{GC}} \quad (60)$$

Using Eq. (58), one obtains:

$$\frac{(KR)^2}{1 - \left(\frac{KR}{2} \right)^2} = \frac{2R}{\ell_{GC}}, \quad (61)$$

which can be solved:

$$\frac{KR}{2} = \sqrt{\frac{R/\ell_{GC}}{R/\ell_{GC} + 2}}. \quad (62)$$

Hence, in contrast with the slit geometry, an explicit expression of K can be derived in general for a cylindrical channel.

4. A few integrals

a. Electrostatic energy \mathcal{E} (per unit length of the channel) Denoting $y = KR/2$,

$$\begin{aligned} \mathcal{E} &= \frac{\varepsilon}{2} \int_0^R 2\pi r dr \left(\frac{dV}{dr} \right)^2 \\ &= \frac{2}{\ell_B \beta} \left[\ln(1 - y^2) + \frac{y^2}{1 - y^2} \right] \end{aligned} \quad (63)$$

Using Eq. (62), \mathcal{E} can be directly written in terms of R/ℓ_{GC} :

$$\mathcal{E} = \frac{2}{\ell_B \beta} \left[\ln \left(\frac{2}{R/\ell_{GC} + 2} \right) + \frac{R}{2\ell_{GC}} \right] \quad (64)$$

b. Ionic density

$$\int_0^R 2\pi r dr n(z) = 2\pi R \frac{|\Sigma|}{q} = \frac{R}{\ell_B \ell_{GC}} \quad (65)$$

5. Low and high surface charge limits

a. Low surface charge When Σ is small enough that $R/\ell_{GC} \ll 1$, Eq. (62) simplifies:

$$KR \approx \sqrt{2R/\ell_{GC}}, \quad (66)$$

which is accurate to within 1% up to $R/\ell_{GC} \approx 0.04$.

Note that when $R/\ell_{GC} \ll 1$, $KR \ll 1$, so that $\psi \approx 0$ and the ion density is approximately homogeneous in the channel:

$$n \approx \frac{K^2}{2\pi\ell_B} = \frac{1}{\pi R \ell_B \ell_{GC}}. \quad (67)$$

This is commonly called the *ideal gas* regime. In practice, the ion density varies by less than 10% over the channel thickness as long as $R/\ell_{GC} < 0.1$.

b. High surface charge When Σ is large enough that $R/\ell_{GC} \gg 1$, Eq. (62) simplifies:

$$KR \approx \frac{2}{1 + \frac{\ell_{GC}}{R}}, \quad (68)$$

which is accurate to within 1% down to $R/\ell_{GC} \approx 7$.

Eventually, when $R/\ell_{GC} \rightarrow \infty$, $KR \rightarrow 2$, and the potential and ion density profiles reach a limit, sometimes referred to as the ‘‘Gouy-Chapman limit’’:

$$\psi(r) = 2 \ln \left[1 - \left(\frac{r}{R} \right)^2 \right], \quad (69)$$

$$n(r) = \frac{2}{\pi\ell_B R^2 \left[1 - \left(\frac{r}{R} \right)^2 \right]^2}. \quad (70)$$

C. General case

In a cylindrical channel, we are not aware of a usable analytical solution for the general case, and the PB equation has to be solved numerically (a Python script to that aim is provided in the appendix, A 2). Nevertheless, like in the slit case, one can define two ratios $r_1 = R/\lambda_D$ and $r_2 = \lambda_D/\ell_{GC}$, which uniquely determine the auxiliary reduced potential $\psi = -\text{sgn}(\Sigma) \times \phi$ expressed as a function of the reduced position $y = r/R$. Different approximate solutions can be written depending on r_1 and r_2 , discussed in the following.

1. Debye-Hückel limit

When the reduced potential $|\psi|$ is small everywhere, the PB equation can be linearized (DH regime).

With the conditions:

$$\left. \frac{d\psi}{dr} \right|_{r=0} = 0 \quad \text{and} \quad \left. \frac{d\psi}{dr} \right|_{r=R} = -\frac{2}{\ell_{GC}},$$

the solution to the linearized PB equation in cylindrical coordinates, $\frac{1}{r} \frac{d}{dr} \left(r \frac{d\psi}{dr} \right) = \psi/\lambda_D^2$, writes:

$$\psi(r) = -\frac{2\lambda_D}{\ell_{GC}} \frac{I_0\left(\frac{r}{\lambda_D}\right)}{I_1\left(\frac{R}{\lambda_D}\right)} = -2r_2 \frac{I_0(r_1 y)}{I_1(r_1)}, \quad (71)$$

where $I_0(x)$ and $I_1(x)$ are the modified Bessel functions of the first kind of order zero and one. The corresponding potential V writes:

$$V(r) = \frac{\Sigma \lambda_D}{\varepsilon} \frac{I_0\left(\frac{r}{\lambda_D}\right)}{I_1\left(\frac{R}{\lambda_D}\right)}. \quad (72)$$

The limits of validity of this approximation will be quantified in section V D.

Electrostatic energy \mathcal{E} (per unit length of the cylindrical channel) With $y = R/\lambda_D$,

$$\begin{aligned} \mathcal{E} &= \frac{\varepsilon}{2} \int_0^R 2\pi r \left(\frac{dV}{dr} \right)^2 dr \\ &= \frac{R^2}{2\beta \ell_{GC}^2} \left[1 - \frac{I_0(y)I_2(y)}{I_1(y)^2} \right]. \end{aligned} \quad (73)$$

2. Homogeneous/parabolic potential limits

a. Homogeneous potential When the EDLs overlap ($r_1 = R/\lambda_D \ll 1$) and for low enough surface charges ($r_1 r_2 = R/\ell_{GC} \ll 1$), the potential and ion densities are almost homogeneous: this is commonly referred to as

the ideal gas limit. In this limit, the ion densities and the auxiliary reduced potential write:

$$\begin{aligned} n_{\pm}^{\text{IG}} &= \mp \frac{\Sigma}{qR} + \sqrt{n_0^2 + \left(\frac{\Sigma}{qR} \right)^2} \\ &= n_0 \left\{ \mp \text{sgn}(\Sigma) \frac{\ell_{Du}}{R} + \sqrt{1 + \left(\frac{\ell_{Du}}{R} \right)^2} \right\}, \end{aligned} \quad (74)$$

$$\psi_{\text{IG}} = -\text{asinh}\left(\frac{\ell_{Du}}{R}\right) = -\text{asinh}\left(\frac{4r_2}{r_1}\right), \quad (75)$$

introducing the Dukhin length $\ell_{Du} = (|\Sigma|/q)/n_0 = 4\lambda_D^2/\ell_{GC}$. The limits of validity of this approximation will be discussed in section V D.

b. Parabolic potential For weaker EDL overlaps, one can expand the solution of the PB equation in series of r/λ_D ; to second order, one obtains [12]:

$$\psi(r) \approx \psi_m + \frac{\sinh(\psi_m)}{4} \left(\frac{r}{\lambda_D} \right)^2. \quad (76)$$

Using $\psi_m = \psi_{\text{IG}}$, one gets:

$$\psi(r) \approx -\text{asinh}\left(\frac{4r_2}{r_1}\right) - \frac{r_2}{r_1} \left(\frac{r}{\lambda_D} \right)^2. \quad (77)$$

However, the ideal gas potential is close to the average potential in the channel, and systematically shifted from the potential in the middle of the channel. The shift can be estimated as:

$$\frac{1}{\pi R^2} \int_0^R -\frac{r_2}{r_1} \left(\frac{r}{\lambda_D} \right)^2 2\pi r dr \approx -\frac{r_1 r_2}{2},$$

and it can be subtracted from ψ_{IG} to obtain a closer approximation to ψ_m :

$$\psi_{\text{IG}}^{\text{cor}} = -\text{asinh}\left(\frac{4r_2}{r_1}\right) + \frac{r_1 r_2}{2}. \quad (78)$$

Overall, a good practical approximation for $\psi(r)$ is:

$$\begin{aligned} \psi(r) &\approx \psi_{\text{IG}}^{\text{cor}} + \frac{\sinh(\psi_{\text{IG}})}{4} \left(\frac{r}{\lambda_D} \right)^2 \\ &= -\text{asinh}\left(\frac{4r_2}{r_1}\right) + \frac{r_1 r_2}{2} - \frac{r_2}{r_1} \left(\frac{r}{\lambda_D} \right)^2. \end{aligned} \quad (79)$$

The limits of validity of this approximation will be discussed in section V D.

3. No co-ion limit

When the EDL extends over the whole channel and for large enough surface charges, co-ions are excluded

from the channel and the PB equation can be solved with counter-ions only, see Sec. VB. The auxiliary reduced potential $\psi(r)$ and the counter-ion density profile $n(r)$ were given by Eq. (57) and by Eq. (59), respectively. Both ψ and n depended on an inverse length K related to the surface charge via Eq. (62).

However, the potential in the middle of the channel was arbitrarily fixed to zero. To reproduce the exact potential, one needs to acknowledge that the channel is connected to an external salt reservoir with salt concentration n_0 and corresponding Debye length λ_D . Moving the reference of potential to the reservoir, $\psi_0 = 0$, the Boltzmann distribution for the counter-ions becomes $n(z) = n_0 e^{-\psi(z)}$, and the PB equation rewrites:

$$\frac{1}{r} \frac{d}{dr} \left(r \frac{d\psi}{dr} \right) = -\frac{1}{2\lambda_D^2} e^{-\psi(r)},$$

$$\text{with } \left. \frac{d\psi}{dr} \right|_{r=0} = 0 \quad \text{and} \quad \left. \frac{d\psi}{dr} \right|_{r=R} = -\frac{2}{\ell_{GC}}.$$

Denoting $KR = r_3$, the solution writes:

$$\psi = 2 \ln \left\{ \frac{r_1}{2r_3} \left[1 - \left(\frac{r_3 y}{2} \right)^2 \right] \right\}, \quad (80)$$

with

$$r_3 = 2 \sqrt{\frac{r_1 r_2}{r_1 r_2 + 2}}. \quad (81)$$

In particular, the potential in the center of the channel is $\psi_m = \psi(y=0) = 2 \ln [r_1/(2r_3)]$. The limits of validity of this approximation will be discussed in section VD.

D. Validity of the approximate solutions

We will in the following bound the regions in the $r_1 - r_2$ diagram where the different approximate solutions can be used safely, see Fig. 4.

1. Thin EDL limit

When the channel radius R is much larger than λ_D , one can neglect the wall curvature at the scale of the EDL, and solve the PB equation for a single planar charged wall.

However this approximation should be taken with caution. Even when the EDL is significantly thinner than the channel radius ($R/\lambda_D > 10$), the planar wall solution only provides a fair description of the exact potential profile. Still, this boundary is represented with a green dashed line in Fig. 2.

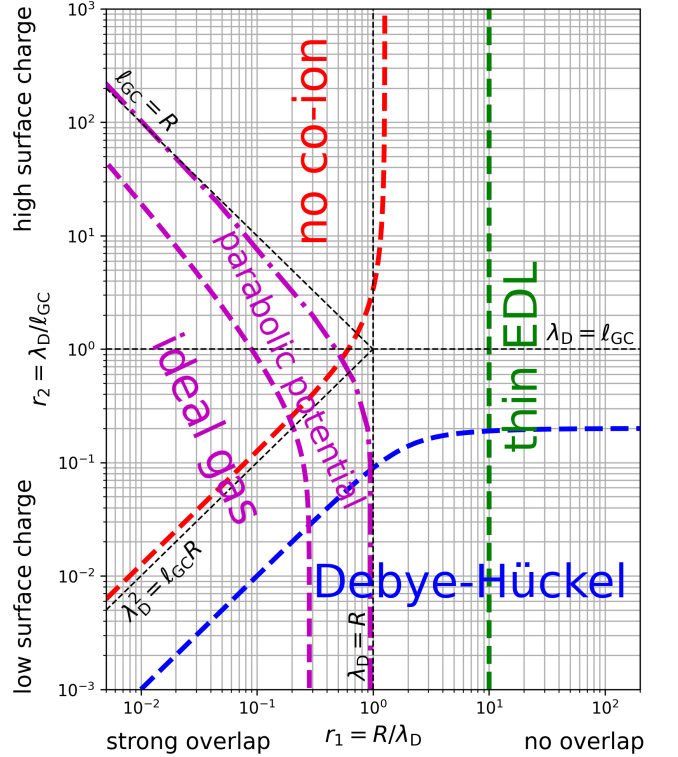


FIG. 4. Domains of validity of the different approximate solutions to the PB equation for an electrolyte solution confined inside a cylindrical channel, as a function of the ratios $r_1 = R/\lambda_D$ and $r_2 = \lambda_D/\ell_{GC}$, where R is the channel radius, λ_D the Debye length, and ℓ_{GC} the Gouy-Chapman length.

2. Debye-Hückel limit

Like in the slit case, the DH potential introduced in Sec. VC1 is an excellent approximation to the exact potential as long as the surface potential, $|\psi_s| = \max(|\psi|) = |\psi(r=R)|$ remains under a (somehow arbitrary) critical value $\psi_c = 0.4$. This corresponds to:

$$r_2 \leq \frac{I_1(r_1)}{I_0(r_1)} \times \frac{\psi_c}{2}. \quad (82)$$

This boundary is represented with a blue dashed line in Fig. 4.

One can then simplify the relation between r_1 and r_2 by considering two limits: for thin EDLs, $r_1 \gg 1$, the DH solution can be used up to $r_2 \leq \psi_c/2$; for overlapping EDLs, $r_1 \ll 1$, the DH solution can be used up to $r_2 \leq r_1 \times \psi_c/4$.

3. Homogeneous/parabolic potential limits

a. *Homogeneous potential (ideal gas)* To estimate the range of validity of the homogeneous potential approximation (see Sec. VC2), one can compare the homogeneous potential value to the next term in a Taylor

series of the potential as a function of R/λ_D , i.e., the parabolic term.

The homogeneous potential writes: $|\psi_{IG}| = \text{asinh}(4r_2/r_1)$, and the maximum difference between the parabolic term and its average value writes: $r_1 r_2/2$. Imposing a maximum ratio θ_c between the two terms, one obtains:

$$r_1 r_2 = 2\theta_c \text{asinh}\left(\frac{4r_2}{r_1}\right). \quad (83)$$

This boundary is represented for $\theta_c = 1\%$ with a purple dashed line in Fig. 4.

b. Parabolic potential The accuracy of the parabolic potential approximation depends crucially on the choice of ψ_m . Using $\psi_m = \psi_{IG}$, the error is approximately the same as the one of the homogeneous potential approximation. In contrast, Eq. (79) approximates the exact potential within 1% over a broader range of parameters, see the purple dashed-dotted line in Fig. 4.

4. No co-ion limit

To determine the limits of applicability of this regime, one can estimate the ratio η between counter-ions and co-ion densities in the middle of the channel:

$$\eta = \frac{n_m^{\text{counter-ion}}}{n_m^{\text{co-ion}}} = \exp\{-2\psi_m\} = \left(\frac{2r_3}{r_1}\right)^4. \quad (84)$$

One can consider that co-ions are efficiently excluded from the channel when η is above a critical value η_c , that we will arbitrarily fix to 100. Combining Eq. (81) and Eq. (84), one can see that $\eta = \eta_c$ corresponds to:

$$r_2 = \frac{2r_1\eta_c^{1/2}}{16 - r_1^2\eta_c^{1/2}}. \quad (85)$$

This boundary is represented with a red dashed line in Fig. 4.

One can simplify the relation between r_1 and r_2 by considering two limits: for small surface charges, $r_2 \ll 1$, the no co-ion approximation can be used for $r_2 \geq r_1\eta_c^{1/2}/8 \approx 1.25r_1$; for large surface charges, $r_2 \gg 1$, the no co-ion approximation can be used for $r_1 \leq 4/\eta_c^{1/4} \approx 1.26$.

VI. COMMON BOUNDARY CONDITIONS

A. Surface charge density and surface potential

At a charged surface, the surface charge density Σ and the surface potential ϕ_s can be linked by expressing the electric field at the wall as a function of the surface charge, Eq. (10). This equation can be solved when the shape of the potential is known, resulting e.g. in the Grahame equation, Eq. (11), for one wall with salt.

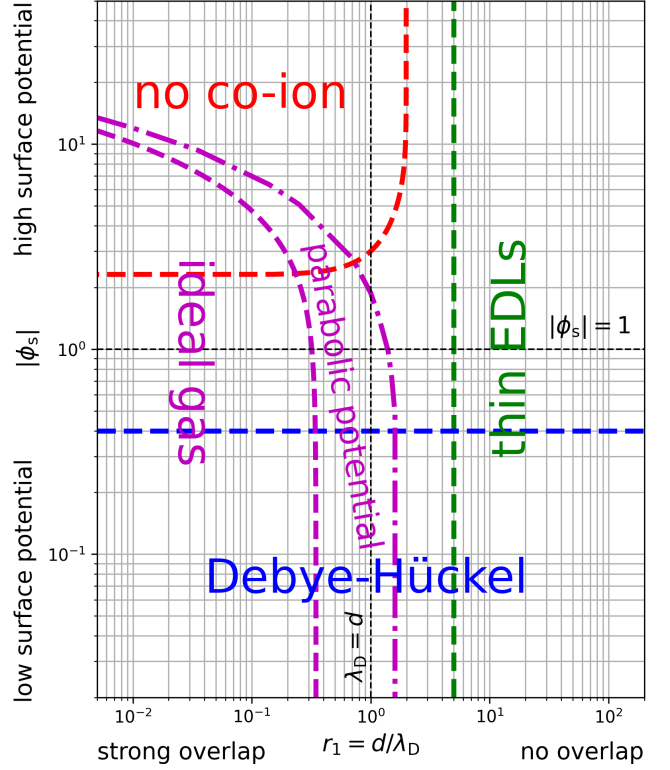


FIG. 5. Domains of validity of the different approximate solutions to the PB equation for an electrolyte solution confined between two planar walls, as a function of $r_1 = d/\lambda_D$ and $|\phi_s|$, where d is the distance between the walls, λ_D the Debye length, and ϕ_s the reduced surface potential.

B. Constant charge

Insulating walls are commonly described using a constant surface charge, i.e., the surface charge density Σ is imposed. This is the boundary condition considered by default in this formulary. The surface potential ϕ_s can then be obtained from interfacial electrostatics, see Sec. VIA.

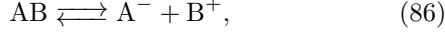
C. Constant potential

In contrast, conducting surfaces are usually described using a constant potential, i.e., the surface potential ϕ_s is imposed. All the results in the formulary can be expressed in terms of the surface potential ϕ_s and/or $\gamma = \tanh(\phi_s/4)$, through the relation between ϕ_s and Σ given by interfacial electrostatics, see Sec. VIA.

The domains of validity of the different approximations can also be represented, e.g. for a slit channel, as a function of $r_1 = d/\lambda_D$ and $|\phi_s|$, see Fig. 5.

D. Charge regulation

Finally, surface charge and potential can be controlled by chemical reactions at the surface, for instance in the presence of ionizable groups at the surface, which can release counter-ions into the solution [16]. We will present here the simple and common case of a single-site dissociation process, described by the reaction:



where AB denotes a neutral surface site that can be ionized, A^- , releasing a counter-ion B^+ in solution (we arbitrarily consider a negatively charged surface, and monovalent ionized sites). This process is characterized by an equilibrium constant K_d through:

$$K_d = \frac{[A^-][B^+]_s}{[AB]}, \quad (87)$$

where $[A^-]$, $[B^+]_s$, and $[AB]$ denote the concentrations of the species at the surface.

Denoting a the average distance between the ionizable sites on the surface, one can relate the fraction of ionized groups φ_A to the surface charge: $\varphi_A = -\Sigma a^2/e$. φ_A is also related to the concentrations of AB and A^- at the surface through: $[A^-]/[AB] = \varphi_A/(1 - \varphi_A)$.

The concentration of B^+ at the interface can then be expressed as a function of the surface potential, and Eq. (87) provides a relation between the surface charge and the surface potential. Formally, denoting n_B^{bulk} the concentration of B^+ in bulk, $[B^+]_s = n_B^{\text{bulk}} \exp(-\phi_s)$, and Eq. (87) can be rewritten:

$$\varphi_A = -\frac{\Sigma a^2}{e} = \frac{1}{1 + \frac{1}{K_d} n_B^{\text{bulk}} \exp(-\phi_s)}. \quad (88)$$

Finally, interfacial electrostatics provides another relation between surface charge and surface potential (e.g. Grahame equation, Eq. (11), for one wall with salt), so that Σ and ϕ_s can be uniquely determined by combining the two equations.

VII. LIMITS OF THE PB FRAMEWORK

In the first molecular layers of liquid close to the wall, the hypotheses underlying the PB equation generally fail. The reader can find detailed discussions on the limits of the PB theory in e.g. Refs. 1–5, 7–10, 17, 18.

Here we will simply present a criterion for the validity of the mean field approximation. The importance of ionic correlations can be quantified by the plasma parameter Γ , see Refs. 19–21, which compares the typical interaction energy between two ions and the thermal energy $k_B T$:

$$\Gamma = \frac{\beta q^2}{4\pi\epsilon d_{\text{ion}}} = \frac{\ell_B}{d_{\text{ion}}}, \quad (89)$$

where d_{ion} is the typical inter-ionic distance.

This typical inter-ionic distance can be related to surface or bulk properties, imposing respectively a critical surface charge density $|\Sigma|^c$ or a critical salt concentration n_0^c above which the applicability of the PB framework should be taken with care.

At the surface, assuming that counter-ions organize into a monolayer screening the surface charge, $1/d_{\text{ion}}^2 = |\Sigma|/q$, and $\Gamma^{\text{surface}} = \sqrt{|\Sigma|\ell_B^2/q}$. Ionic correlations cannot be neglected when $\Gamma^{\text{surface}} > 1$, see Refs. 19, 20, corresponding to:

$$|\Sigma| > |\Sigma|^c = \frac{q}{\ell_B^2} = \frac{(4\pi\epsilon/\beta)^2}{(Ze)^3}, \quad (90)$$

where the last expression highlights the strong impact of the ion valence Z on $|\Sigma|^c$. For monovalent ions in water at 300 K, $|\Sigma|^c \sim 330 \text{ mC/m}^2$, but for divalent ions it drops to $\sim 40 \text{ mC/m}^2$.

In bulk, because the total ionic concentration is twice the salt concentration, the inter-ionic distance is $d_{\text{ion}} = (2n_0)^{-1/3}$, and $\Gamma^{\text{bulk}} = (2n_0\ell_B^3)^{1/3}$. Ionic correlations cannot be neglected when $\Gamma^{\text{bulk}} > 1$, see Refs. 19, 20, corresponding to:

$$n_0 > n_0^c = \frac{1}{2\ell_B^3} = \frac{(4\pi\epsilon/\beta)^3}{2(Ze)^6}. \quad (91)$$

For a monovalent salt in water at 300 K, $n_0^c \sim 2 \text{ M}$, but for a divalent salt it drops to $\sim 30 \text{ mM}$.

Finally, it is important to note that, for monovalent ions in water at room temperature, $\ell_B \sim 7 \text{ \AA}$ is greater than the ionic size, so that there will be no steric repulsion effects when $\Gamma = \ell_B/d_{\text{ions}} < 1$.

ACKNOWLEDGMENTS

The authors thank E. Trizac and O. Vinogradova for their feedback.

-
- [1] J. Lyklema, *Fundamentals of Interface and Colloid Science: Vol. II - Solid/Liquid Interfaces* (Academic press, 1995).
 [2] R. J. Hunter, *Foundations of colloid science* (Oxford University Press, 2001).

- [3] J. Israelachvili, *Intermolecular and Surface Forces* (Academic Press, 2011).
 [4] A. Delgado, F. González-Caballero, R. Hunter,

- L. Koopal, and J. Lyklema, Measurement and interpretation of electrokinetic phenomena, *Journal of Colloid and Interface Science* **309**, 194 (2007).
- [5] R. Schoch, J. Han, and P. Renaud, Transport phenomena in nanofluidics, *Reviews of Modern Physics* **80**, 839 (2008).
- [6] L. Bocquet and E. Charlaix, Nanofluidics, from bulk to interfaces, *Chem. Soc. Rev.* **39**, 1073 (2010).
- [7] R. Hartkamp, A.-L. Bianco, L. Fu, J.-F. Dufrêche, O. Bonhomme, and L. Joly, Measuring surface charge: Why experimental characterization and molecular modeling should be coupled, *Current Opinion in Colloid & Interface Science* **37**, 101 (2018).
- [8] N. Kavokine, R. R. Netz, and L. Bocquet, Fluids at the Nanoscale: From Continuum to Subcontinuum Transport, *Annual Review of Fluid Mechanics* **53**, 377 (2021).
- [9] D. Andelman, Electrostatic Properties of Membranes: The Poisson-Boltzmann Theory, in *Handbook of Biological Physics*, Vol. 1B (Elsevier, 1995) pp. 603–642.
- [10] T. Markovich, D. Andelman, and R. Podgornik, Charged Membranes: Poisson-Boltzmann theory, DLVO paradigm and beyond, *arXiv preprint arXiv:1603.09451* (2016).
- [11] G. Weisbuch and M. Guéron, Une longueur d’échelle pour les interfaces chargées, *Journal de Physique* **44**, 251 (1983).
- [12] E. F. Silkina, E. S. Asmolov, and O. I. Vinogradova, Electro-osmotic flow in hydrophobic nanochannels, *Physical Chemistry Chemical Physics* **21**, 23036 (2019).
- [13] R. E. Rice and F. H. Horne, Analytical solutions to the linearized poisson—boltzmann equation in cylindrical coordinates for different ionic—strength distributions, *Journal of Colloid and Interface Science* **105**, 172 (1985).
- [14] P. Berg and K. Ladipo, Exact solution of an electro-osmotic flow problem in a cylindrical channel of polymer electrolyte membranes, *Proceedings of the Royal Society A: Mathematical, Physical and Engineering Sciences* **465**, 2663 (2009).
- [15] P. Berg and J. Findlay, Analytical solution of the Poisson–Nernst–Planck–Stokes equations in a cylindrical channel, *Proceedings of the Royal Society A: Mathematical, Physical and Engineering Sciences* **467**, 3157 (2011).
- [16] T. Markovich, D. Andelman, and R. Podgornik, Charge regulation: A generalized boundary condition?, *EPL (Europhysics Letters)* **113**, 26004 (2016).
- [17] D. J. Bonthuis and R. R. Netz, Beyond the Continuum: How Molecular Solvent Structure Affects Electrostatics and Hydrodynamics at Solid–Electrolyte Interfaces, *The Journal of Physical Chemistry B* **117**, 11397 (2013).
- [18] S. Faucher, N. Aluru, M. Z. Bazant, D. Blankschtein, A. H. Brozena, J. Cumings, J. Pedro de Souza, M. Elimielech, R. Epsztein, J. T. Fourkas, A. G. Rajan, H. J. Kulik, A. Levy, A. Majumdar, C. Martin, M. McEldrew, R. P. Misra, A. Noy, T. A. Pham, M. Reed, E. Schwegler, Z. Siwy, Y. Wang, and M. Strano, Critical Knowledge Gaps in Mass Transport through Single-Digit Nanopores: A Review and Perspective, *The Journal of Physical Chemistry C* **123**, 21309 (2019).
- [19] Y. Levin, Electrostatic correlations: from plasma to biology, *Reports on Progress in Physics* **65**, 1577 (2002).
- [20] Y. Levin, E. Trizac, and L. Bocquet, On the fluid–fluid phase separation in charged-stabilized colloidal suspensions, *Journal of Physics: Condensed Matter* **15**, S3523 (2003).
- [21] L. Joly, C. Ybert, E. Trizac, and L. Bocquet, Liquid friction on charged surfaces: from hydrodynamic slippage to electrokinetics., *The Journal of Chemical Physics* **125**, 204716 (2006).

Appendix A: Numerical solution with Python

The Python codes listed below solve numerically the PB equation in the slit and cylindrical geometries, using the `solve_bvp` function of the `SciPy` package. The script files are included in the sources of this archive.

1. Slit channel

This code computes and plots the auxiliary reduced potential $\psi = -\text{sgn}(\Sigma) \times \phi$ as a function of the reduced position z/d in a slit channel with walls located at $z = -d/2$ and $z = d/2$ (see Sec. IV C), for a broad range of values of $r_1 = d/\lambda_D$ and $r_2 = \lambda_D/\ell_{GC}$.

In order to use the `solve_bvp` function, one needs to convert the PB equation into a first order system of ordinary differential equations subject to two-point boundary conditions:

$$\frac{d^2\psi}{dz^2} = \frac{1}{\lambda_D^2} \sinh\{\psi\} \quad \text{with} \quad \left. \frac{d\psi}{dz} \right|_{z=0} = 0 \quad \text{and} \quad \left. \frac{d\psi}{dz} \right|_{z=d/2} = -\frac{2}{\ell_{GC}}$$

$$x = z/d, \quad y_0 = \psi, \quad r_1 = d/\lambda_D, \quad r_2 = \lambda_D/\ell_{GC} \quad \Rightarrow \quad \begin{cases} y'_0 = y_1 \\ y'_1 = r_1^2 \sinh(y_0) \end{cases} \quad \text{with} \quad \begin{cases} y_1(0) = 0 \\ y_1(1/2) = -2r_1 r_2 \end{cases}$$

Listing 1. PB_slit_num.py

```
#!/usr/bin/env python3
```

```

# -*- coding: utf-8 -*-

r1 = 5.
r2 = 5.

import numpy as np
import matplotlib.pyplot as plt
from scipy.integrate import solve_bvp

# y0 = psi
# x = z/d

# Right-hand side of the system:
# y0' = y1
# y1' = r1^2 sinh(y0)
def fun(x, y):
    return np.vstack((y[1], r1**2*np.sinh(y[0])))

# Boundary conditions:
# y1(left) = 0
# y1(right)+2r1r2 = 0
def bc(ya, yb):
    return np.array([ya[1], yb[1]+2.0*r1*r2])

# Solving for x in [0;0.5]
x = np.linspace(0., 0.5, 10000)
y = np.zeros((2, x.size))

# Initial guess for the potential profile
r1init = 1.
r3init = 3.135322030076839 # r2init = 1000
y[0] = 2.*np.log(r1init/(2.*r3init)*np.cos(r3init*x))

# Calling solve_bvp
res = solve_bvp(fun, bc, x, y, tol=1.e-6, max_nodes=5000000)

x_plot = np.linspace(0., 0.5, 500)
y_plot = res.sol(x_plot)[0]
plt.plot(x_plot, y_plot, label='numerical')

plt.legend()
plt.xlabel(r"$z/d$")
plt.ylabel(r"$\psi$")

plt.show()

```

2. Cylindrical channel

This code computes and plots the auxiliary reduced potential $\psi = -\text{sgn}(\Sigma) \times \phi$ as a function of the reduced position r/R in a cylindrical channel of radius R (see Sec. VC), for a broad range of values of $r_1 = R/\lambda_D$ and $r_2 = \lambda_D/\ell_{GC}$.

In order to use the `solve_bvp` function, one needs to convert the PB equation into a first order system of ordinary differential equations subject to two-point boundary conditions:

$$\frac{d^2\psi}{dr^2} + \frac{1}{r} \frac{d\psi}{dr} = \frac{1}{\lambda_D^2} \sinh\{\psi\} \quad \text{with} \quad \left. \frac{d\psi}{dr} \right|_{r=0} = 0 \quad \text{and} \quad \left. \frac{d\psi}{dr} \right|_{r=R} = -\frac{2}{\ell_{GC}}$$

$$x = r/R, \quad y_0 = \psi, \quad r_1 = R/\lambda_D, \quad r_2 = \lambda_D/\ell_{GC} \quad \Rightarrow \quad \begin{cases} y_0' = y_1 \\ y_1' = r_1^2 \sinh(y_0) - y_1/x \end{cases} \quad \text{with} \quad \begin{cases} y_1(0) = 0 \\ y_1(1) = -2r_1r_2 \end{cases}$$

Listing 2. PB.cyl_num.py

```
#!/usr/bin/env python3
# -*- coding: utf-8 -*-

r1 = 5.
r2 = 5.

import numpy as np
import matplotlib.pyplot as plt
from scipy.integrate import solve_bvp

# y0 = psi
# x = r/R

# Right-hand side of the system:
# y0' = y1
# y1' = r1^2 sinh(y0) - y1/x
def fun(x, y):
    return np.vstack((y[1], r1**2*np.sinh(y[0]) - y[1]/x))

# Boundary conditions:
# y1(left) = 0
# y1(right) + 2r1r2 = 0
def bc(ya, yb):
    return np.array([ya[1], yb[1] + 2.0*r1*r2])

# Solving for x in ]0;1]
x = np.linspace(1.e-6, 1., 10000)
y = np.zeros((2, x.size))

# Initial guess for the potential profile
r1init = 1.
r3init = 1.9980029950087341 # r2init = 1000
y[0] = 2.*np.log(r1init/(2.*r3init)*(1.-(r3init*x/2)**2))

# Calling solve_bvp
res = solve_bvp(fun, bc, x, y, tol=1.e-6, max_nodes=5000000)

x_plot = np.linspace(0., 1., 500)
y_plot = res.sol(x_plot)[0]
plt.plot(x_plot, y_plot, label='numerical')

plt.legend()
plt.xlabel(r"$r/R$")
plt.ylabel(r"$\psi$")

plt.show()
```